Three-dimensional magnetic structures and rare-earth magnetic ordering in Nd_2CuO_4 and Pr_2CuO_4

M. Matsuda, K. Yamada, K. Kakurai, H. Kadowaki,* T. R. Thurston, and Y. Endoh
Department of Physics, Tohoku University, Aoba-ku, Sendai 980, Japan

Y. Hidaka
Nippon Telegraph and Telephone Opto-Electronics Laboratories, Nippon Telegraph and Telephone Corporation, Tokai, Ibaraki 319-11, Japan

R. J. Birgeneau and M. A. Kastner
Department of Physics, Massachusetts Institute of Technology, Cambridge, Massachusetts 02139

P. M. Gehring, A. H. Moudden,† and G. Shirane
Physics Department, Brookhaven National Laboratory, Upton, New York 11973
(Received 29 March 1990)

The three-dimensional (3D) magnetism present in Nd_2CuO_4 and Pr_2CuO_4 has been examined in neutron-scattering experiments. Antiferromagnetic long-range order of the Cu^{2+} moments develops below $T_N=255$ K in both compounds. In Nd_2CuO_4 a series of magnetic phase transitions in which the Cu^{2+} spins reorient has also been observed below T_N, while in Pr_2CuO_4 the 3D Cu^{2+} spin structure is stable. No changes in the crystalline structure of Nd_2CuO_4 associated with the spin-reorientation transitions were found. Induced ordering of the rare-earth magnetic moments has been observed in both compounds. The Nd^{3+} (Pr^{3+}) magnetic moments align parallel (antiparallel) to Cu^{2+} moments which are nearest neighbors along the c axis, and the ordered moments of the rare-earth ions were determined to be $\sim 1.3\mu_B$ for Nd^{3+} at 0.4 K and $\sim 0.08\mu_B$ for Pr^{3+} at 8 K. The temperature-dependent Pr^{3+} moment is shown to be proportional to the Cu^{2+} moment times the bulk susceptibility. In this paper we also discuss the role of the XY anisotropy in the 3D ordering.

I. INTRODUCTION

Soon after the discovery[1] of electron carrier superconductors such as $Nd_{2-x}Ce_xCuO_4$ and $Pr_{2-x}Ce_xCuO_4$, the magnetic properties of the parent compounds were investigated.[2-11] A number of properties similar to those[12] of La_2CuO_4 were discovered. These common properties include (i) three-dimensional (3D) antiferromagnetic long-range order (LRO) originating from Cu^{2+} $S=\frac{1}{2}$ spins with Néel temperatures in the range 250–325 K, (ii) Cu^{2+} intraplanar exchanges which are very large, >100 meV, and interplanar exchanges which are very small, $<10^{-2}$ MeV, and (iii) highly inelastic 2D spin correlations at temperatures well above the 3D magnetic transition.

However, there are several essential differences in the magnetism of the parent compounds of the hole and electron carrier systems. One of the most obvious differences is that the weak ferromagnetism found[13] in La_2CuO_4 does not exist in the electron carrier systems because the latter are tetragonal. Another difference occurs because the L^{3+} ions (L = Nd, Pr, Gd, etc.) in the electron-doped systems have localized moments which can order,[10] whereas the La^{3+} ions in La_2CuO_4 are nonmagnetic. Finally, the 3D ordered spins in Nd_2CuO_4 undergo a complicated series of reorientation transitions.[4-6]

In this paper we present the results of neutron-scattering studies of the 3D magnetism in Nd_2CuO_4 and Pr_2CuO_4. Several neutron-scattering experiments on these materials have already been published.[4-9] In this work we extend previous results by examining the behavior of Pr_2CuO_4 and, because there has been some controversy about the nature of the magnetic structures found in Nd_2CuO_4, we also present a thorough quantitative discussion of this topic. In addition, we discuss the results of high-resolution x-ray-scattering experiments where a search for structural anomalies in Nd_2CuO_4 associated with magnetic transitions was performed.

The organization of this paper is as follows: In Sec. II a brief discussion of the crystal characteristics and experimental configurations is presented. Experimental results on Nd_2CuO_4 and Pr_2CuO_4 are given in Secs. III and IV respectively. Last, in Sec. V we discuss the implications of our results including especially an extensive discussion of the 3D ordering in various lamellar CuO_2 insulating antiferromagnets.

II. EXPERIMENTAL DETAILS

Single crystals of Nd_2CuO_4 and Pr_2CuO_4 were grown from a nonstoichiometric CuO-rich solution using techniques similar to those discussed in Hidaka *et al.*[14] Typical crystal dimensions were $\sim 15\times15\times1.5$ mm,[3] and lattice parameters at 300 K were ($a=3.941$ Å, $c=12.16$ Å) for Nd_2CuO_4 and ($a=3.962$ Å, $c=12.21$ Å) for Pr_2CuO_4 (tetragonal notation). Experiments were performed on both as-grown and heat-treated samples. Two different heat treatments were performed on two different Nd_2CuO_4 crystals; in one, the sample was heated in Ar at 950 °C for 15 h and in the other, the sample was heated in oxygen at 600° C for 200 h. The only heat treatment done in the case of Pr_2CuO_4 was an anneal in Ar at 950 °C for 10 h. The procedures used in these heat treatments were identical to those previously performed on La_2CuO_4 described in Ref. 15.

Neutron-scattering experiments were carried out on the Tohoku University Neutron Spectrometer (TUNS) and the ND-I spectrometer of the Institute for Solid State Physics of Tokyo University, both of which are installed at the JRR-2 reactor of the Japan Atomic Energy Research Institute in Tokai. A single pyrolytic graphite (PG) monochromator was used in the TUNS experiments, and a double PG monochromator was used in the ND-I experiments. Contamination from higher-order reflec- tions was suppressed by using a PG filter. The incident neutron energy for all experiments described here was 13.7 MeV ($k=2.57$ Å^{-1}). A closed-cycle ^{4}He refrigerator was used for the experiments above 8 K and a ^{3}He cryostat for those below 8 K. The crystals were mounted with the [010] axis vertical to the scattering plane so that magnetic peaks with Miller indices $(h,0,1)$ could be measured.

X-ray-scattering measurements were carried out at Brookhaven National Laboratory. A conventional anode source and synchrotron beam line X-22 were used in these experiments.

In a previous paper[4] by a subset of the authors the magnetic reflections were indexed using the $I4/mmm$ space group. In the present paper we have indexed the magnetic reflections using the magnetic space group $FAmm'm'$,[7] which has a unit cell obtained by a $\sqrt{2}\times\sqrt{2}$ expansion and 45° rotation of the basal plane of the $I4/mmm$ chemical unit cell. Consequently, magnetic reflections such as $(h/2,h/2,1)$ discussed in Ref. 4 correspond to $(h,0,1)$ in this paper.

III. Nd_2CuO_4 EXPERIMENTS

We begin with a review of the successive magnetic phase transitions found in Nd_2CuO_4. This behavior is illustrated in Fig. 1. Magnetic Bragg reflections indicative of a La_2NiO_4-type structure develop below $T_N=255$ K (phase I). As the temperature is decreased further, drastic changes in the peak intensities occur at $T_1=75$ K, $T_2=30$ K and possibly at ~ 20 K. The data presented here clearly demonstrate that at least three magnetically ordered phases occur in Nd_2CuO_4; phase I ($T_1<T<T_N$), phase II ($T_2<T<T_1$), and phase III ($T<T_2$). In phase I and phase II only the Cu^{2+} spin orientations are shown explicitly in Fig. 2. The data shown in the inset of Fig. 1 suggest that a fourth phase may even exist at temperatures below 0.8 K.

In order to determine the spin structure in these phases, the integrated intensities of a number of magnetic peaks were obtained from $\theta-2\theta$ scans. Room-temperature intensities were subtracted in this procedure to remove higher-order contamination, and an overall intensity scale factor was defined by adjusting the calculated (1,0,1) intensity to the observed intensity in phase I. For the Nd^{3+} and Pr^{3+} ions, we used a form factor calculated

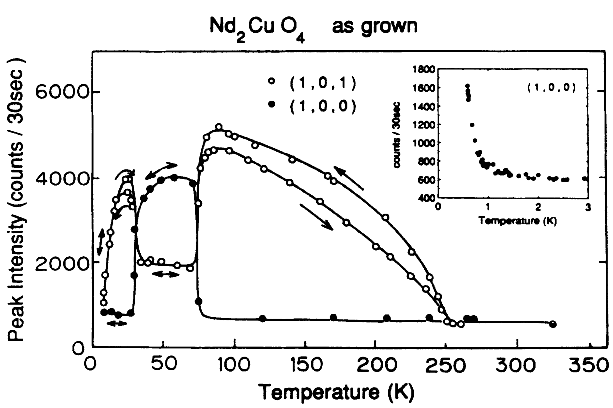

FIG. 1. Temperature evolution of the (1,0,0) and (1,0,1) 3D antiferromagnetic peak intensities in as-grown Nd_2CuO_4.

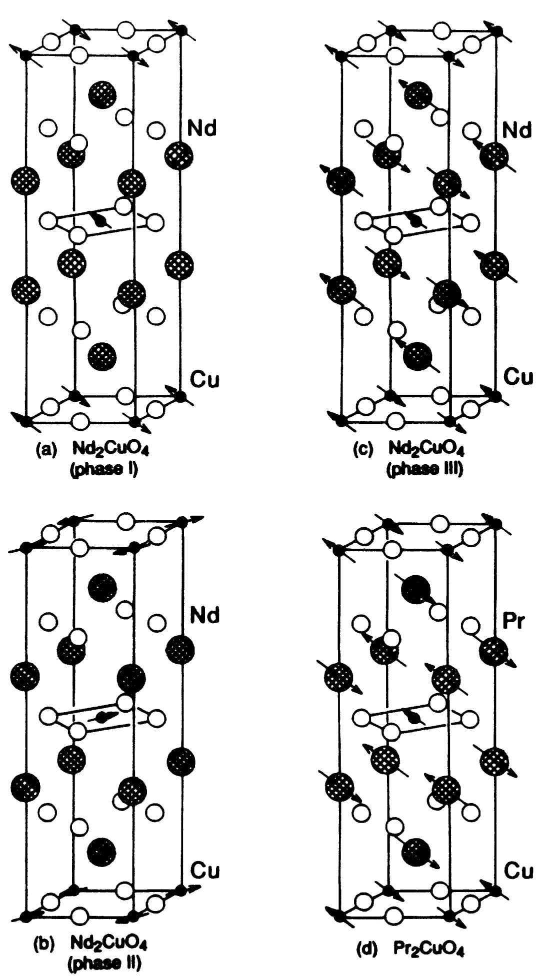

FIG. 2. Proposed 3D magnetic structures: (a) Nd_2CuO_4 (phase I, La_2NiO_4-type), (b) Nd_2CuO_4 (phase II, La_2CuO_4-type), (c) Nd_2CuO_4 (phase III), and (d) Pr_2CuO_4. Note that, in Nd_2CuO_4 phases I and II, the Nd^{3+} moments have not been explicitly determined.

TABLE I. Observed and calculated intensities of magnetic Bragg reflections at $T=100$ K (phase I), $T=50$ K (phase II), and $T=23$ and 8 K (phase III) on Nd_2CuO_4.

	$T=100$ K (phase I)		$T=50$ K (phase II)		$T=23$ K (phase III)		$T=8$ K (phase III)	
(h,k,l)	I_{obs}	I_{calc}	I_{obs}	I_{cal}	I_{obs}	I_{calc}	I_{obs}	I_{calc}
(1,0,0)	4.8	0.0	196.2	155.1	−5.7	0.0	2.4	0.0
(1,0,1)	205.6	205.6	67.9	52.6	137.3	118.0	7.6	3.2
(1,0,2)	82.6	70.9	181.7	147.0	76.6	54.9	44.6	22.5
(1,0,3)	104.4	114.1	52.6	78.6	205.1	227.6	650.7	705.0
(1,0,4)	46.3	76.4	102.0	96.8	24.7	32.5	2.4	8.9
(1,0,5)	82.6	87.8	86.0	75.1	99.6	90.5	103.0	108.4
(1,0,6)	95.7	72.0	80.7	80.6	162.9	121.7	440.8	330.6
(3,0,0)	2.7	0.0	28.4	36.2	−15.7	0.0	12.6	0.0
(3,0,1)	41.1	40.1	12.1	35.9	28.4	18.5	10.8	1.0
(3,0,2)	2.0	3.4	48.9	36.2	−2.0	2.4	−11.2	0.6
$M_{Cu}(\mu_B)$	0.4		0.4		0.4		0.4	
$M_{Nd}(\mu_B)$	0		0		0.08		0.28	

from a dipole approximation.[16] For the Cu^{2+} magnetic form factor, La_2CuO_4 experimental[17] values and interpolations to the experimental values were utilized. We mention that reasonable agreement between the calculated and observed intensities of the (1,0,5) and (1,0,6) peaks could only be achieved by including a small oscillatory component in the Q dependence of the Cu^{2+} magnetic form factor. This behavior is evident in the experimental form factor and it has some theoretical justification.[18]

A detailed comparison between observed and calculated intensities, the results of which are presented in Table I, leads to the conclusion that phase transitions in which the Cu^2 spins reorient occur at both T_1 and T_2. However, the change in peak intensities that is evident below 20 K could be best explained by a model in which the Nd^{3+} ordered moment increases significantly. In Fig. 2 we show our proposed spin structure for each phase. As we shall discuss later in this paper in the context of Pr_2CuO_4, once long-range order is achieved on the Cu^{2+} sites, there will be a small moment induced on the Nd^{3+} sites; however, we did not attempt to determine these moments in phases I and II. We mention that a spin structure for phase III identical to ours has recently been proposed by Rosseinsky *et al.*[8] In Fig. 2 we have assumed that the spins are collinear, although as discussed elsewhere[19] our measurements cannot distinguish between noncollinear and collinear structures. An illustration of the La_2NiO_4-type noncollinear structure is shown in Fig. 3. The noncollinear structure is derived from the collinear structure by superimposing the two different collinear domains on every other layer. A similar noncollinear structure can be constructed from the two domains of the collinear La_2CuO_4 structure.

From the structure analysis presented in Table I, we found the moment per Cu^{2+} spin in Nd_2CuO_4 to be $0.4\pm0.1\mu_B$ at 8 K. We mention that this value for the 3D Cu^{2+} ordered moment is apparently somewhat smaller than that of La_2CuO_4, $\sim0.5\mu_B$ (Ref. 12) although the disagreement is within the errors.

We now describe phases I–III in more detail. The structure in phase I can be described well with the Cu^{2+} moments ordered in a La_2NiO_4-type structure[20] with τ// [100] and S//[100], where τ and S denote the antiferromagnetic propagation vector and spin vector, respectively. In the transition that occurs at T_1, (75 K), the spins rotate from S//[100] to S⊥[100], so that the new phase has a spin structure identical to that of La_2CuO_4.[12] In La_2CoO_4, a spin reorientation similar to the 75 K transition in Nd_2CuO_4 is triggered by a structural phase transition.[21] In Nd_2CuO_4, however, no evidence for a distortion from the $I4/mmm$ structure has been observed at the magnetic phase transition or any other temperature. In Fig. 4 we show the temperature dependence of the lattice constants in Nd_2CuO_4 measured in x-ray-scattering experiments. An upper limit of the change in $(b-a)/(b+a)$ over the temperature range 280–10 K was found to be 4×10^{-5}. Further, no superlattice peaks such as (1,0,0), (1,0,1), or (1,0,2) were detected over this same temperature range, even when using the intense synchrotron source. This issue is also discussed by Takada *et al.*,[22] who conclude that previous reports[5] of a structural peak at the (1,0,3) position were, in fact,

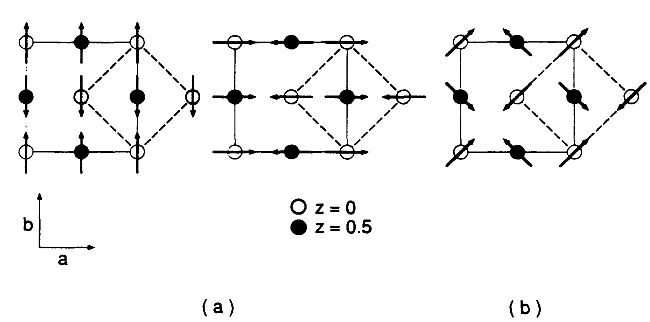

FIG. 3. (a) The two magnetic domains of the collinear La_2NiO_4 structure and (b) the corresponding noncollinear structure with equal admixtures of the two domains.

caused by higher-order contamination of the incident beam. It is, of course, possible that different samples could behave differently. The deviation from the linear temperature dependence of the lattice constants at ~75 K could possibly be associated with the magnetic transition at this same temperature.

We actually obtain the best agreement between observed intensities and calculations in phase II with two distinct models. In the first we assume a mixture of ~10% La_2NiO_4-type structure and ~90% La_2CuO_4-type structure. This phenomenon may be related to the hysteresis shown in Fig. 1. Our experiments show that the thermal hysteresis evident in phases I and III only occurs when coming from phase II. This suggests that the observed hysteresis is related to the coexistence of the two spin structures in phase II. The La_2NiO_4-type structure in the predominantly La_2CuO_4-type phase II could then be understood as being the result of "misreorientations" between the spins of adjacent CuO_2 planes; that is, the spins in one plane rotate clockwise and in the next plane counterclockwise by 90°. These misorientations would appear to persist into phases I and III. Within this context, we expected to see diffuse scattering from these stacking faults; no diffuse scattering has been observed within the instrumental resolution. A second explanation for the measured intensities is that a single phase exists but in this phase the Cu^{2+} spins in alternating layers rotate by an angle which is less than 90°. Our experiment cannot distinguish between the first and second possibilities.

At T_2 (30 K), the Cu^{2+} spins return back to the [100] direction. The Cu^{2+} structure is identical to that of phase I; in addition, the participation of Nd^{3+} moments in the magnetic order can now be clearly seen. The most direct evidence for Nd^{3+} ordering is shown in Fig. 5, where an increase in the intensity of the (1,0,3) reflection at ~3 K can be seen. This temperature is reasonably close to the Nd^{3+} ordering temperature deduced by Markert *et al.*[10] from specific-heat measurements. To demonstrate explicitly that these anomalous temperature dependencies arise from the progressive ordering of the Nd^{3+} spins, consider the intensity data for $T=23$ and 8 K shown in Table I. In spite of the huge difference in intensities of some reflections at the two temperatures, we obtained good agreement between calculated and observed intensity values by adjusting only the magnitude of the Nd^{3+} moment. In a similar analysis we deter-

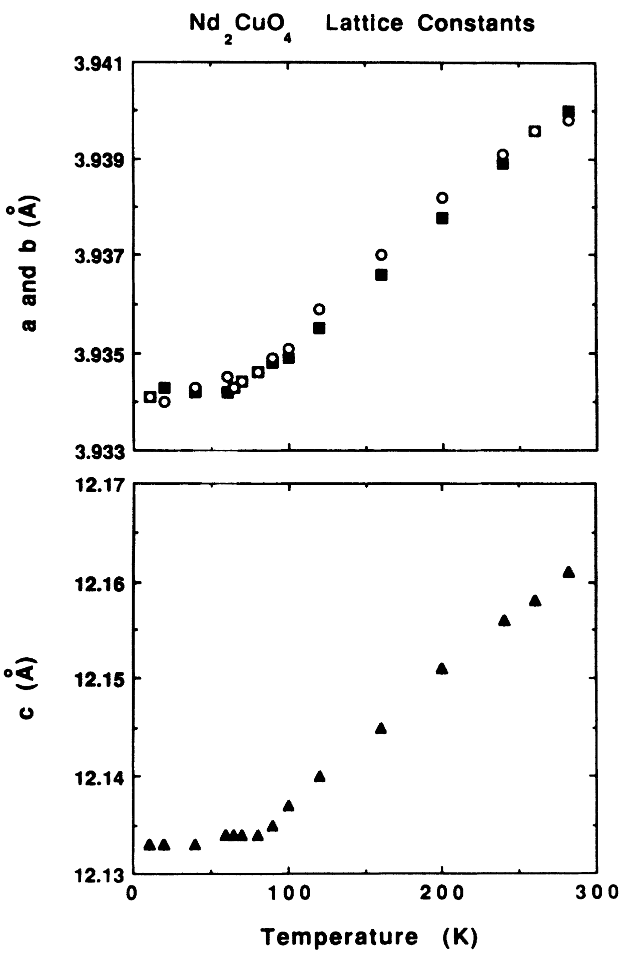

FIG. 4. Temperature dependence of the lattice constants in Nd_2CuO_4.

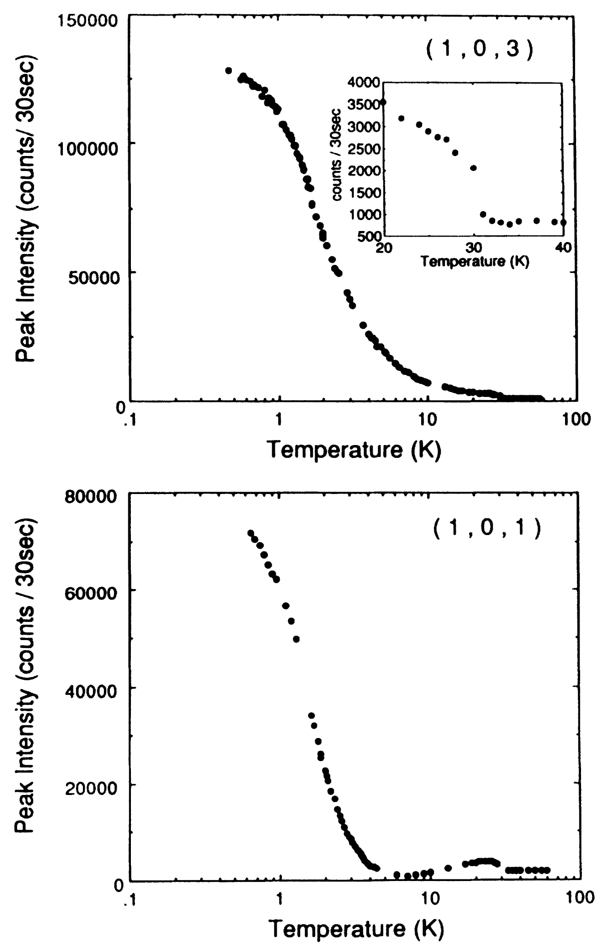

FIG. 5. Temperature dependence of the (1,0,1) and (1,0,3) peak intensities in Nd_2CuO_4 at low temperatures.

mined the Nd^{3+} magnetic moment to be $1.3\mu_B$ at 0.4 K. This value is considerably reduced from the free-ion Nd^{3+} value of $3.27\mu_B$; presumably this differences arises primarily from crystal-field effects.[23]

The ordering of the Nd^{3+} moments also affects the (1,0,1) peak intensity; in this case, however, the intensity actually decreases between ~20 and 8 K. The difference in the behavior of the (1,0,3) and (1,0,1) peak intensities arises from differences in the structure factors. A simple calculation shows that the intensities of these two peaks are proportional to

$$\begin{aligned} I(1,0,1) &\sim (M_{\mathrm{Cu}} f_{\mathrm{Cu}} - 1.2 M_{\mathrm{Nd}} f_{\mathrm{Nd}})^2 , \\ I(1,0,3) &\sim (M_{\mathrm{Cu}} f_{\mathrm{Cu}} + 1.9 M_{\mathrm{Nd}} f_{\mathrm{Nd}})^2 , \end{aligned} \quad (1)$$

where M and f represent the ordered staggered moment and form factor of the Cu^{2+} and Nd^{3+} ions. The decrease in the (1,0,1) intensity is thus seen to be an interference effect, so that both measurements indicate that the Nd^{3+} ions order.

The Nd^{3+} ordering transition below 3 K is actually rather broad. Moreover, the (1,0,3) intensity data in Fig. 5 show that ordering of the Nd^{3+} spins begins at much higher temperatures. Indeed, as noted above, Table I indicates that the Nd^{3+} moment is already $0.08\mu_B$ at 23 K. The character of the scattering therefore suggests that the Nd^{3+} ions exhibit a moment at high temperatures which is induced by coupling to the Cu^{2+} moments as one expects on symmetry grounds alone. The increase in the (1,0,3) intensity at ~3 K would then reflect an incipient spontaneous transition in the Nd^{3+} ions due to their own spin-spin interactions. We mention that the increase in the (1,0,3) intensity at 30 K shown in the inset of Fig. 5 most likely arises from a reorientation of the Nd^{3+} spins which occurs simultaneously with the Cu^{2+} spin reorientation. Clearly, the Nd^{3+} ions must have an induced moment for all temperatures below the Cu^{2+} ordering temperature, 255 K, although for reasons discussed below this induced moment is appreciable only below ~30 K.

We now consider the increase of the (1,0,0) intensity below 0.8 K shown in the inset of Fig. 1. Although our current data are rather limited, the most probable cause of this intensity increase is the canting of the Nd^{3+} spins along the c axis while keeping the Cu^{2+} spins fixed in the c plane. If this conjecture is correct, then the cant angle is estimated to be 4° at 0.4 K. Note that the latest high-field measurements by Date showing a spin-flip transition at a lower field of around 5 T also indicate canting of the Nd moments.

Experiments identical to those described above were performed on the heat-treated Nd_2CuO_4 samples. No significant differences in the transition temperatures or character of the transitions between phases I, II, and III were observed. This behavior is quite different from that of La_2CuO_4, where identical heat treatments drastically affected the 3D and 2D magnetic order.[15] Whether the behavior found in Nd_2CuO_4 is intrinsic or a reflection of the inability of oxygen to diffuse out from single crystals under the conditions described is currently unknown.

IV. Pr_2CuO_4

In contrast to the complicated behavior of Nd_2CuO_4, the Cu^{2+} moments in Pr_2CuO_4 only ordered in a La_2NiO_4-type structure from 255 K ($=T_N$) to 0.4 K. This same magnetic structure has been previously proposed from neutron-diffraction measurements on powders[7] and single crystals.[9] In these previous studies no magnetic contribution from the Pr^{3+} ions was taken into account; however, we have found that inclusion of a small magnetic moment on the Pr^{3+} ions considerably improves the agreement between the observed and the calculated intensities. The structure we propose for this magnetic order is shown in Fig. 2(d). We mention that the Pr^{3+} moments in Pr_2NiO_4 also order.[24]

To illustrate the necessity of including a Pr^{3+} ordered moment, a comparison between intensity calculations with and without Pr^{3+} ordering and the experimentally observed intensities is given in Table II. The effects of the Pr^{3+} moments are especially observable at $(1,0,3n)$ reflections with n = integer because the z parameter of the Pr^{3+} site is nearly $\frac{1}{3}$ so that the phase factor $\cos(2\pi z l)$ for the Pr^{3+} moments is large at $l=3n$. The

TABLE II. Observed and calculated intensities of magnetic Bragg reflections on Pr_2CuO_4.

	$T=8$ K			$T=150$ K		
(h,k,l)	I_{obs}	I_{calc}	I_{calc}	I_{obs}	I_{calc}	I_{calc}
(1,0,0)	0.8	0.0	0.0	1.2	0.0	0.0
(1,0,1)	205.6	205.6	205.6	113.8	113.8	113.8
(1,0,2)	60.6	58.7	71.6	37.5	36.2	39.6
(1,0,3)	23.3	25.9	114.1	32.4	36.3	63.1
(1,0,4)	102.7	88.7	76.2	54.5	45.4	42.2
(1,0,5)	60.4	55.7	87.8	45.2	39.7	48.6
(1,0,6)	25.0	23.8	71.7	24.5	25.5	39.7
(3,0,0)	1.9	0.0	0.0	1.0	0.0	0.0
(3,0,1)	43.3	44.7	40.0	23.8	23.4	22.2
(3,0,2)	11.7	2.9	3.4	6.8	1.8	1.9
$M_{\mathrm{Cu}}(\mu_B)$		0.4	0.48		0.33	0.36
$M_{\mathrm{Pr}}(\mu_B)$		0.08			0.03	

Pr^{3+} and Cu^{2+} ordered moments at 8 K are found to be $\sim 0.08\mu_B$ and $\sim 0.40\mu_B$, respectively, from this analysis. We note that Nd_2CuO_4 and Pr_2CuO_4 both have the same low-temperature 3D ordered Cu^{2+} moment.

The temperature dependence of the Cu^{2+} and Pr^{3+} 3D ordered moments can be found from the (1,0,1) and (1,0,3) peak intensities shown in Fig. 6. For the structure shown in Fig. 2(d), the (1,0,1) and (1,0,3) peak intensities are proportional to

$$I(1,0,1) \sim (M_{\mathrm{Cu}} f_{\mathrm{Cu}} + 1.2 M_{\mathrm{Pr}} f_{\mathrm{Pr}})^2 \; , \qquad (2)$$
$$I(1,0,3) \sim (M_{\mathrm{Cu}} f_{\mathrm{Cu}} - 1.9 M_{\mathrm{Pr}} f_{\mathrm{Pr}})^2 \; ,$$

where M and f are ordered staggered moments and form factors for the Cu^{2+} and Pr^{3+} ions. Thus, the decrease in the (1,0,3) peak intensity below ~ 100 K in Pr_2CuO_4 arises from an interference effect similar to that which occurs at the (1,0,1) peak in Nd_2CuO_4, and the anomalous increase of the (1,0,1) intensity evident at ~ 150 K can be attributed to the progressive ordering of the Pr^{3+} moments rather than a change in the Cu^{2+} spin structure. We show the temperature dependence of the 3D ordered moments of the Cu^{2+} and Pr^{3+} ions separately in Fig. 7. These data were obtained from the intensity data shown in Fig. 6 and the above equations. In this analysis we have set the low-temperature ordered moments of the Cu^{2+} and Pr^{3+} ions at exactly $0.40\mu_B$ and $0.08\mu_B$, respectively; the error bars in Fig. 7 do not reflect the possible systematic error which will arise if these values for the low-temperature ordered moment are not exact. As we shall discuss quantitatively below, the Pr^{3+} ions order because of coupling to the Cu^{2+} ions. The line through the Pr^{3+} moment in Fig. 7 represents the prediction of a mean-field treatment of coupled $Cu^{2+}-Pr^{3+}$ ions which we discuss below.

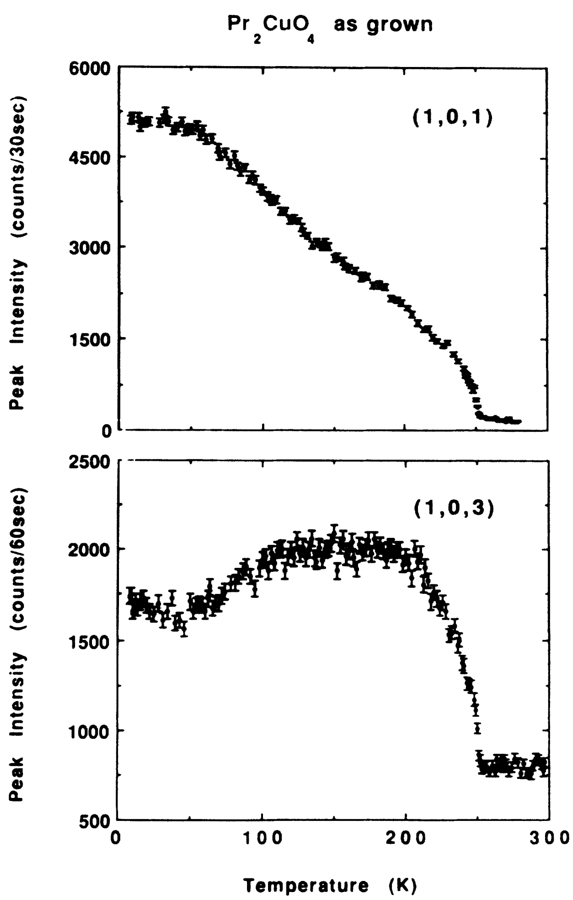

FIG. 6. Temperature dependence of the (1,0,1) and (1,0,3) peak intensities in Pr_2CuO_4.

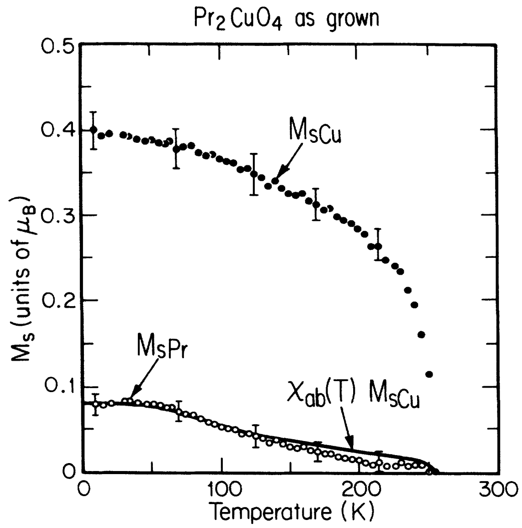

FIG. 7. Temperature dependence of the Cu^{2+} and Pr^{3+} 3D ordered moments in Pr_2CuO_4. The solid line is the product of the measured bulk susceptibility and the copper moment normalized to $0.08\mu_B$ at $T=0$.

As in the case of Nd_2CuO_4, experiments carried out on the heat-treated sample of Pr_2CuO_4 revealed no significant departures from the behavior of as-grown samples in the 3D magnetism. It is not currently known whether this behavior is intrinsic or whether it arises from the inability of oxygen to diffuse out from the single crystal under the conditions described.

V. DISCUSSION

A. The rare-earth magnetic moments

We discuss first the magnetic moments of the Nd^{3+} and Pr^{3+} ions in these systems. The existence of a permanent magnetic moment on the Nd^{3+} ions at low temperatures has been corroborated in magnetization[25] and specific-heat[10] measurments; this result can also be easily understood within the framework of a crystal-field treatment of the $4f$ electrons.[23] In Pr_2CuO_4, however, the existence of an induced Pr^{3+} moment has only been revealed by the present diffraction experiments. Magnetization[9,10,25] experiments have suggested that the crystal field quenches the Pr^{3+} moment; the level scheme determined by neutron inelastic scattering measurements supports this interpretation.[9] The small magnitude of the Pr^{3+} moment revealed in our experiments confirms that the ground state is of singlet character but that a small admixture of higher-lying states giving a net magnetic moment occurs because of the coupling to the Cu^{2+} ions.

The rare-earth moments in both the Nd_2CuO_4 and Pr_2CuO_4 systems begin to participate in the 3D long-range order at the Cu^{2+} Néel temperature. As discussed earlier, this occurs because the rare-earth moments interact with the Cu^{2+} spins. Although the antiferromagnetic order of the Cu^{2+} spins and tetragonal symmetry of the systems inhibit nearest-neighbor Cu^{2+}-(rare-earth) exchange processes, second-nearest-neighbor exchange can be appreciable. In a mean-field treatment where the Cu^{2+} ions, through the Cu^{2+}-(rare-earth) exchange, exert an effective magnetic field on the rare-earth ions, the moment of the rare earth (RE) as a function of temperature is given by

$$\langle M_{\mathrm{RE}} \rangle \sim \chi_{ab} J \langle M_{\mathrm{Cu}} \rangle \ . \tag{3}$$

Here χ_{ab} is the single-ion paramagnetic susceptibility of the rare-earth ions within the a-b plane and J is the Cu^{2+}-(rare-earth) interaction energy. Because the Cu^{2+} ions are strongly correlated antiferromagnetically, the measured bulk susceptibilities of both Nd_2CuO_4 and Pr_2CuO_4 are dominated by the rare-earth ions. Using susceptibility data from, for example, Allenspach *et al.*,[9] one can easily check this model in Pr_2CuO_4; the line in Fig. 7 through the Pr^{3+} moment data was computed from Cu^{2+} moment and susceptibility data via Eq. (3). The magnitude of the Pr^{3+} moment was fixed at $0.08\mu_B$ at low temperatures and there is no other adjustable parameter. Clearly the agreement between this simple theory and experiment is excellent. A similar analysis could be carried out for Nd_2CuO_4; we have not done this because the spin-reorientation transition and ordering of the Nd^{3+} ions via their own spin-spin interactions introduce additional complications. We nonetheless point out that the low-temperature susceptibility of Nd_2CuO_4 is dominated by the lowest Kramers doublet, which produces a Curie-Weiss behavior where the susceptibility rises dramatically below ~ 30 K.[10] This explains why the Nd^{3+} moment is appreciable only at low temperatures.

B. Three-dimensional ordering temperatures

One of the striking features of the lamellar CuO_2 insulating antiferromagnets is that the Néel temperatures are closely similar in a large number of materials both tetragonal and orthorhombic, frustrated and unfrustrated. In this section we discuss the probable origins of this phenomenon with emphasis on Pr_2CuO_4 and Nd_2CuO_4. All of these CuO_2 materials are characterized by a strong, nearly isotropic, nearest-neighbor exchange coupling within the sheets and much weaker exchange coupling between the sheets. Further, as may be seen in Fig. 1, in the $I4/mmm$ structure the exchange interaction between nearest-neighbor planes is fully frustrated, thus significantly reducing the effective interplanar coupling.

As discussed originally in Ref. 26, in such lamellar materials 2D spin correlations develop progressively with decreasing temperature within the layers and there is then a crossover to 3D behavior when the interplanar coupling between correlated regions becomes of order kT. In mean-field theory, this heuristic argument implies

$$J_\perp S^2 \left[\frac{M_s}{M_0} \right]^2 \left[\frac{\xi_{2D}(T_N)}{a} \right]^2 \sim k_B T_N \ , \tag{4}$$

where $J_\perp$ is interplanar interaction, M_s is the sublattice magnetization, $M_0 = g\mu_B$ and $\xi_{2D}(T_N)$ is the 2D correlation length at T_N in the absence of the 3D coupling. Avaiable 2D correlation length data[27,28] for Pr_2CuO_4, Nd_2CuO_4, and La_2CuO_4 ($T_N = 245$ K) are shown in Fig. 8. The solid lines are all of the form

$$K(rlu) = K_0 e^{-2\pi\rho_s/kT} \tag{5}$$

as predicted by Chakravarty, Halperin, and Nelson[29] (CHN) for the 2D $S=\frac{1}{2}$ Heisenberg model at low temperatures. Here K is the inverse correlation length.

For La_2CuO_4, $2\pi\rho_s$ was fixed at the spin-wave value, $2\pi\rho_s = 0.576$, $\hbar c/a = 1500$ K using Aeppli *et al.*'s[30] value $\hbar c = 0.85$ eV Å for a sample with $T_N = 265 \pm 5$ K. This choice served to fix the prefactor in Eq. (5) at $K_0 = 0.36$, which agrees with the CHN estimate within the combined experimental and theoretical uncertainties. The curves for Nd_2CuO_4 and Pr_2CuO_4 correspond to Eq. (5) with K_0 fixed at 0.36 and $2\pi\rho_s = 1370$ and 1160 K, respectively.[27] These correspond to effective nearest-neighbor exchange constants of 137 ± 8, 126 ± 5, and 106 ± 7 MeV for La_2CuO_4 ($T_N = 245$ K), Nd_2CuO_4 ($T_N = 255$ K), and Pr_2CuO_4 ($T_N = 255$ K), respectively. These value are in reasonable agreement with those deduced from two-magnon Raman scattering measurements.[31]

If one assumes ideal 2D Heisenberg behavior, then the correlation lenghs at T_N should be ~ 290, 130, and 60 lattice constants in La_2CuO_4, Nd_2CuO_4, and Pr_2CuO_4, respectively. For La_2CuO_4 from Eq. (4), this implies $J_\perp \sim 3\times10^{-3}$ MeV. This may be compared with the value $J_\perp = 7\times10^{-3}$ MeV deduced by Thio *et al.*[13] from their magnetization measurements on a sample with

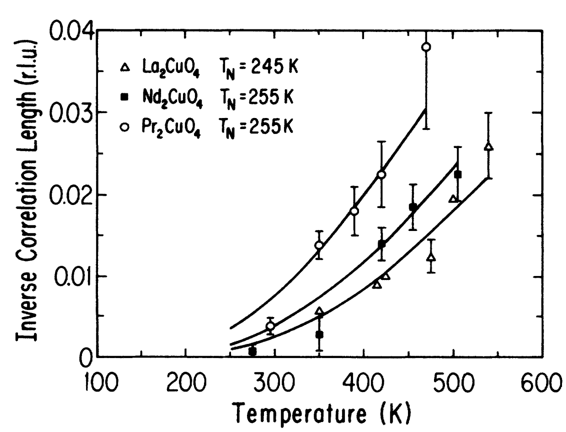

FIG. 8. Temperature dependence of the 2D antiferromagnetic inverse correlation lengths in La_2CuO_4, Nd_2CuO_4, and Pr_2CuO_4. The solid lines correspond to Eq. (5) with $2\pi\rho_s = 1500$, 1370, and 1160 K, respectively.

$T_N \sim 240$ K [including the zero-point correction factor $(M_s/M_0)^2$ which was not considered in Ref. 13]. This agreement is clearly quite satisfactory and would seem to justify the above general approach. However, as discussed by Thio *et al.*,[13] this large between-plane coupling in La_2CuO_4 explicitly arises from the orthorhombic distortion; that is, the exact cancellation of the exchange fields between nearest-neighbor planes is lifted and there is a small, but nonzero, exchange interaction between the nearest-neighbor planes which drives the 3D ordering. It should be mentioned that a similar situation obtains for $YBa_2Cu_3O_6$.[32] In that case, the coupling between the bilayers separated by the CuO chains is weak, ~ 0.013 MeV, but still adequate to account for the high-ordering temperature without the detailed consideration of terms beyond the Heisenberg exchange coupling. Specifically, in stoichiometric La_2CuO_4 the Néel temperature is ~ 320 K while in $YBa_2Cu_3O_{6.0}$, $T_N \sim 415$ K. As we have noted above, the ordering temperature in La_2CuO_4 is reasonably accounted for by Eqs. (4) and (5). The interplanar coupling in $YBa_2Cu_3O_{6.0}$ (Ref. 32) is about four times larger than that in La_2CuO_4 necessitating that, from Eq. (4), the 2D correlation length at T_N in the absence of the 3D coupling should be a factor of 2 smaller. As is evident from the La_2CuO_4 data around 415 K in Fig. 8, this, in fact, appears to be the case.

It is immediately evident from Fig. 8 that these arguments will fail for Pr_2CuO_4 and Nd_2CuO_4. Specifically, because of the tetragonal symmetry, the effective interlayer coupling is 2 orders of magnitude weaker in these two materials compared with that in La_2CuO_4 or $YBa_2Cu_3O_6$. From Eq. (4) this would require $\xi_{2D}(T_N)$ to be an order of magnitude larger in the tetragonal materials compared with its value in La_2CuO_4. The Heisenberg curves in Fig. 8 imply the exact opposite behavior. In discussing the resolution of this conundrum, it is useful to consider, in addition, the material $Sr_2CuO_2Cl_2$ which has been studied by Vaknin *et al.*[33] $Sr_2CuO_2Cl_2$ has the tetragonal La_2CuO_4 structure albeit with the LaO layers replaced by SrCl. Two-magnon Raman measurements[31] show that the nearest-neighbor in-plane exchange in $Sr_2CuO_2Cl_2$ is identical to that in Pr_2CuO_4 and Nd_2CuO_4 to within the errors. Thus, the 2D correlations should exhibit the same behavior as that shown in Fig. 8 for the latter two materials. Vaknin *et al.*[33] find $T_N = 251\pm$ K in their single crystal. It is simplest to discuss $Sr_2CuO_2Cl_2$ first since it contains no magnetic rare-earth ions. $Sr_2CuO_2Cl_2$ orders in the La_2CuO_4 structure; that is, with the spin direction in the CuO_2 plane and perpendicular to the antiferromagnetic propagation direction. Vaknin *et al.*[33] have shown that this 3D structure is preferred by the interplanar magnetic dipole interactions. Further, they find for the dipolar energy a value of $\sim 2\times10^{-6}$ MeV. This corresponds to a $J_\perp$ of $\sim 7\times10^{-6}$ MeV in our notation. Using Eq. (4), one finds that this necessitates $\xi_{2D}(T_N)/a \sim 3000$. This may be compared with the pure 2D Heisenberg model prediction of $\xi_{2D}(251\ \text{K})/a \simeq 100$. Clearly, the pure 2D Heisenberg model fails by a very large factor.

The situation for Pr_2CuO_4 and Nd_2CuO_4 is more complicated because of the presence of the rare-earth ions. We emphasize, however, that the rare-earth–copper intersublattice coupling is again fully frustrated (see Fig. 2). Both Pr_2CuO_4 and Nd_2CuO_4 order at T_N in the La_2NiO_4-type magnetic structure with the spin vector along the antiferromagnetic propagation vector. Presumably this ordering must be preferred by the rare-earth–copper interplanar coupling which then overrules the copper-copper interplanar dipolar interaction. The rare-earth–copper interaction involves both the magnetic dipole-dipole coupling and anisotropic exchange. Because of the very small rare-earth moments near T_N ($\sim 0.01\mu_B$), we expect the interplanar rare-earth–copper coupling to be of the same order of magnitude as the interplanar Cu-Cu interaction. This expectation is confirmed by the behavior in Nd_2CuO_4. It seem clear, therefore, that the net interplanar interactions in Pr_2CuO_4 and Nd_2CuO_4 are comparable to that in $Sr_2CuO_2Cl_2$. This, in turn, necessitates that $\xi_{2D}(T_N)/a \simeq 3000$ for Pr_2CuO_4 and Nd_2CuO_4 in explicit disagreement with the predictions of the 2D Heisenberg model as illustrated in Fig. 8.

The probable resolution of this conundrum is straightforward. We have so far considered only the 2D Heisenberg exchange term. However, due to the tetragonal, rather than cubic, point symmetry around the Cu^{2+} ions, the interaction Hamiltonian in the CuO_2 layers actually has the form

$$H - \sum_{\langle nn \rangle} [J_{xy}^{nn}(S_i^x S_{i+\delta}^x + S_i^y S_{i+\delta}^y) + J_{zz}^{nn} S_i^z S_{i+\delta}^z] \tag{6}$$

with $J_{xy}^{nn} > J_{zz}^{nn}$. In La_2CuO_4 there is, in addition, an antisymmetric exchange term due to the local rotations of the CuO_6 octahedra.[13] We shall not discuss the consequences of that term explicitly here. This anisotropic exchange is conveniently represented as a reduced anisotropy field $h^A = (J_{xy}^{nn} - J_{zz}^{nn})/J_{xy}^{nn}$. In La_2CuO_4, Peters *et al.*[34] find $h^A = 4\times10^{-5}$; Thio *et al.*[13] find a similar value from a study of the spin-flop transition. In $YBa_2Cu_3O_{6.0}$ from the data of Tranquada *et al.*,[32] we deduce $h^A \simeq 2\times10^{-4}$. In both cases, this 2D *XY* anisotropy is of the same order as the between-plane coupling. Thus, in these two materials, the double crossovers from 2D to 3D and Heisenberg to *XY* behavior should occur simultaneously.

In each of Pr_2CuO_4, Nd_2CuO_4, and $Sr_2CuO_2Cl_2$ because of the frustration, the reduced interplanar coupling is only of order 3×10^{-8}. However, because of the fourfold O coordination of the Cu^{2+} ions, we expect the *XY* anisotropies in these materials to be larger than that in $YBa_2Cu_3O_{6.0}$, that is $h^A \gtrsim 2\times10^{-4}$. Thus, in these materials there should be well-separated crossovers from 2D Heisenberg to 2D *XY* behavior and then from 2D *XY* to a 3D *XY* transition. The crossover to 2D *XY* behavior should occur when $h^A\xi^2 \sim 1$, which, in this case, implies a 2D correlation length of order 50 lattice constants.

We thus expect that the 3D Néel transition in frustrated tetragonal CuO_2 materials will occur at a temperature which is very close to the 2D Kosterlitz-Thouless (KT) transition[35] temperature of the system described by Eq. (6). Unfortunately, there is rather little quantitative information available for this Hamiltonian. For $h_A \gtrsim 0.2$. Loh et al.[36] find $T_N^{KT} \sim 0.45\ J_{xy}^{nn} \simeq 630$ K. More recent simulations by Ding and Makivić[37] for the pure $S=\frac{1}{2}$ 2D XY model give $T_N^{KT} \sim 0.35 J_{xy}^{nn} \sim 500$ K. This therefore represent an upper limit to the CuO_2 2D phase-transition temperature. For h_A very small, one expects

$$T_N^{KT} \sim 4\pi\rho_s / \ln(C/h^A)$$

with $C \sim 8$. This explicitly assumes that the Kosterlitz-Thouless transition will occur shortly after the crossover to 2D XY behavior. Using the values for $2\pi\rho_s$ quoted above and assuming h^A is between 10^{-3} and 10^{-4} in the tetragonal CuO_2 materials with four-fold oxygen coordination, this gives T_N^{KT} of order 230–290 K. These values bracket the observed phase-transition temperatures of ~ 255 K in each of Pr_2CuO_4, Nd_2CuO_4, and $Sr_2CuO_2Cl_2$. We believe, therefore, that the close proximity of the phase-transition temperatures in these materials arises from the fact that the J_{nn}'s are similar and T_N^{KT} depends only logarithmically on the XY anisotropy.

In order to test this model, various neutron-scattering measurements are required. First, one should measure the spin-wave gap and thence h_A in each of the materials. Second, the crossover from 2D Heisenberg to 2D XY behavior should be directly observable through the temperature dependence of K and from the geometry of the 2D critical scattering. Indeed, if we are correct, then these materials, and most especially, $Sr_2CuO_2Cl_2$, should provide ideal examples of quantum Kosterlitz-Thouless transitions.[35,36]

Finally, we comment briefly on the spin-orientation transitions in Nd_2CuO_4. As discussed above, the 3D ordering is determined by interplanar couplings which are of relative order 10^{-7}–10^{-8}. Further, this coupling itself involves a competition between the $Cu^{2+}-Cu^{2+}$ and $Nd^{3+}-Cu^{2+}$ interplanar interactions with the $Nd^{3+}-Cu^{2+}$ couplings prevailing near T_N. As the temperature is decreased below T_N, the relative populations of the Nd^{3+} crystal-field levels, and thence the $Nd^{3+}-Cu^{2+}$ interaction, will change. Given the very small net interplanar couplings, this could very easily cause a change in the energy balance between the competing structures thus generating the observed transitions. Unfortunately, these ideas must remain speculative since quantitative predictions of such effects are far beyond our current understanding of the quantum chemistry of these materials.

ACKNOWLEDGMENTS

We would like to thank our colleagues at Tohoku University, Nippon Telegraph and Telephone (NTT), Brookhaven, and Massachusetts Institute of Technology (MIT) for useful discussions. We are especially grateful to Amnon Aharony, Vic Emery, Brooks Harris, and Sunil Sinha for extensive discussions of the 3D ordering. Two of the authors (K.K. and A.H.M.) would like to thank the members of the neutron-scattering group at Brookhaven National Laboratory for their hospitality during their stay. This work was supported by the U.S.-Japan Cooperative Neutron Scattering Program. The work at Tohoku University was supported by a Grant-In-Aid for Science Research from the Japanese Ministry of Education, Science and Culture. The work at Brookhaven National Laboratory was supported by the Division of Material Science, U.S. Department of Energy under Contract No. DE-AC02-76CH00016. The work at Massachusetts Institute of Technology was supported by the National Science Foundation under Contracts Nos. DMR85-01856 and DMR87-19217.

*Permanent address: Institute for Solid State Physics, University of Tokyo, Roppongi, Minato-ku, Tokyo 106, Japan.

†Permanent address: Laboratoire Leon Brillouin, CEN Saclay, 91191 Gif-sur-Yvette, CEDEX, France.

[1]Y. Tokura, H. Takagi, and S. Uchida, Nature (London) **377**, 345 (1989); H. Takagi, S. Uchida, and Y. Tokura, Phys. Rev. Lett. **62**, 1197 (1989).

[2]G. M. Luke, B. J. Sternlieb, Y. J. Uemura, J. H. Brewer, R. Kadono, R. F. Kiefl, S. R. Kreitzman, T. M. Riseman, J. Gopalakrishnan, A. W. Sleight, M. A. Subramanian, S. Uchida, H. Takagi, and Y. Tokura, Nature (London) **338**, 49 (1989).

[3]S. Sugai, T. Kobayashi, and J. Akimitsu, Phys. Rev. B **40**, 2686 (1989).

[4]Y. Endoh, M. Matsuda, K. Yamada, K. Kakurai, Y. Hidaka, G. Shirane, and R. J. Birgeneau, Phys. Rev. B **40**, 7023 (1989).

[5]S. Skanthakumar, H. Zhang, T. W. Clinton, W-H. Li, J. W. Lynn, Z. Fisk, and S-W. Choeng, Physica C **160**, 124 (1989); J. W. Lynn, I. W. Sumarlin, S. Skanthakumar, W.-H. Li, R. N. Shelton, J. L. Peng, Z. Fisk, and S-W. Cheong, Phys. Rev. B **41**, 2569 (1990); S. Skanthakumar, H. Zhang, T. W. Clinton, I. W. Sumarlin, W-H. Li, J. W. Lynn, Z. Fisk, and S-W. Cheong (unpublished).

[6]J. Akimitsu, H. Sawa, T. Kobayashi, H. Fujiki, and Y. Yamada, J. Phys. Soc. Jpn. **58**, 2646 (1989).

[7]D. E. Cox, A. I. Goldman, M. A. Subramanian, J. Gopalakrishnan, and A. W. Sleight, Phys. Rev. B **40**, 6998 (1989).

[8]M. J. Rosseinsky, K. Prassides, and P. Day, J. Chem. Soc. Chem. Commun. **22**, 1734 (1989).

[9]P. Allenspach, S-W. Cheong, A. Dommann, P. Fischer, Z. Fisk, A. Furrer, H. R. Ott, and B. Rupp, Z. Phys. B **77**, 185 (1989).

[10]M. F. Hundley, J. D. Thompson, S-W. Cheong, Z. Fisk, and S. B. Oseroff, Physica C **158**, 109 (1989); J. T. Markert, E. A. Early, T. Bjomholm, S. Ghamaty, B. W. Lee, J. J. Neumeier, R. D. Price, G. L. Seaman, and M. B. Maple, Physica C **158**, 178 (1989).

[11]P. E. Sulewski, P. A. Fleury, K. B. Lyons, S-W. Cheong, and Z. Fisk, Phys. Rev. B **41**, 225 (1990).

[12]R. J. Birgeneau and G. Shirane, in *Physical Properties of High Temperature Superconductors I*, edited by D. M. Ginsberg (World-Scientific, Singapore 1989), and reference therein.

[13]Tineke Thio, T. R. Thurston, N. W. Preyer, P. J. Picone, M. A. Kastner, H. P. Jenssen, D. R. Gabbe, C. Y. Chen, R. J. Birgeneau, and A. Aharony, Phys. Rev. B **38**, 905 (1988); Tineke Thio, C. Y. Chen, B. S. Freer, D. R. Gabbe, H. P.

Jenssen, M. A. Kastner, P. J. Picone, N. W. Preyer, and R. J. Birgeneau, *ibid.* **41**, 231 (1990).
[14]Y. Hidaka, Y. Enomoto, M. Suzuki, M. Oda, and T. Murakami, J. Cryst. Growth **85**, 581 (1987).
[15]K. Yamada, E. Kudo, Y. Endoh, Y. Hidaka, M. Oda, M. Suzuki, and T. Murakami, Solid State Commun. **64**, 753 (1987).
[16]A. J. Freeman and J. P. Desclaux, J. Magn. Magn. Mater. **12**, 4 (1979).
[17]T. Freltoft, G. Shirane, S. Mitsuda, J. P. Remeika, and A. S. Cooper, Phys. Rev. B **37**, 137 (1988).
[18]T. C. Leung, X. W. Wang, and B. N. Harmon, Phys. Rev. B **37**, 384 (1988).
[19]K. Yamada, K. Kakurai, and Y. Endoh, Physica C **165**, 131 (1990).
[20]G. Aeppli and D. J. Buttrey, Phys. Rev. Lett. **61**, 203 (1988).
[21]K. Yamada, M. Matsuda, Y. Endoh, B. Keimer, R. J. Birgeneau, S. Onodera, J. Mizusaki, T. Matsuura, and G. Shirane, Phys. Rev. B **39**, 2336 (1989).
[22]K. Takada, Y. Watanabe, K. Yamada, and Y. Endoh, Physica C **166**, 203 (1990).
[23]P. A. Alekseev, I. Yu. Arnold, S. E. Voinova, M. G. Zemlyanov, V. N. Lazukov, V. G. Orlov, P. P. Parshin, and I. P. Sadikov (unpublished).
[24]T. Fernadez-Diaz, J. Rodriguez-Carvajal, J. L. Martinez, G. Fillion, F. Fernandez, and R. Saez-Puche (unpublished).
[25]R. Saez-Puche, M. Norton, T. R. White, and W. S. Glausinger, J. Solid State Chem. **50**, 281 (1983).
[26]R. J. Birgeneau, H. J. Guggenheim, and G. Shirane, Phys. Rev. B **1**, 2211 (1970).
[27]T. R. Thurston, M. Matsuda, K. Kakurai, K. Yamada, Y. Endoh, R. J. Birgeneau, P. M. Gehring, Y. Hidaka, M. A. Kastner, T. Murakami, and G. Shirane, Phys. Rev. Lett. **65**, 263 (1990).
[28]K. Yamada, K. Kakurai, Y. Endoh, T. R. Thurston, M. A. Kastner, R. J. Birgeneau, G. Shirane, Y. Hidaka, and T. Murakami, Phys. Rev. B **40**, 4557 (1990).
[29]S. Chakravarty, B. I. Halperin, and D. R. Nelson, Phys. Rev. B **39**, 2344 (1989).
[30]G. Aeppli, S. M. Hayden, H. A. Mook, Z. Fisk, S-W. Cheong, D. Rytz, J. P. Remeika, G. P. Espinosa, and A. S. Cooper, Phys. Rev. Lett. **62**, 2052 (1989).
[31]S. Sugai, S. Shamoto, and M. Sato, Phys. Rev. B **38**, 6436 (1988); S. Sugai, T. Kobayashi, and J. Akimitsu, *ibid.* **40**, 2686 (1989); Solid State Commun. **74**, 599 (1990); Y. Tokura, S. Koshihara, T. Arima, H. Takagi, S. Ishibashi, T. Ido, and S. Uchida, Phys. Rev. B **41**, 11 657 (1990); S. L. Cooper, G. A. Thomas, A. J. Millis, P. E. Sulewski, J. Orenstein, D. H. Rapkine, S-W. Cheong, and P. L. Trevor (unpublished).
[32]J. M. Tranquada, G. Shirane, B. Keimer, S. Shamoto, and M. Sato, Phys. Rev. B **40**, 4503 (1989).
[33]D. Vaknin, S. K. Sinha, C. Stassis, L. L. Miller, and D. C. Johnston, Phys. Rev. B **41**, 1926 (1990).
[34]C. J. Peters, R. J. Birgeneau, M. A. Kastner, H. Yoshizawa, Y. Endoh, J. Tranquada, G. Shirane, Y. Hidaka, M. Oda, M. Suzuki, and T. Murakami, Phys. Rev. B **37**, 9761 (1988).
[35]J. M. Kosterlitz and D. J. Thouless, J. Phys. C **6**, 1181 (1973).
[36]E. Loh, Jr., D. J. Scalapino, and P. M. Grant, Phys. Scr. **32**, 327 (1985).
[37]H.-Q. Ding and M. S. Makivić, Phys. Rev. B **42**, 6827 (1990).